

# A Robust Flexible Electrochemical Gas Sensor Using Room Temperature Ionic Liquid

Xiaoyi Mu, *Student Member, IEEE*, Zhe Wang, Xiangqun Zeng, and Andrew J. Mason, *Senior Member, IEEE*

**Abstract**—This paper introduces a robust electrochemical gas sensor featuring room temperature ionic liquid (RTIL) as electrolyte and porous polytetrafluoroethylene as a flexible substrate. Using a planar-electrodes-on-permeable-membrane structure, a flexible RTIL sensor with 9.6 mm<sup>2</sup> sensing area is microfabricated. The sensor's response to oxygen is measured, achieving sensitivity of 0.48  $\mu\text{A}/\%$  O<sub>2</sub>, a linearity of 0.997 R<sup>2</sup> in range of 0%–21% O<sub>2</sub>, and limit of detection of 0.08% O<sub>2</sub>. The reported sensor structure and fabrication process enable realization of sensor arrays for multi-gas monitoring in a low power, miniaturized, and wearable system platform.

**Index Terms**—Gas sensor, flexible sensor, electrochemical sensor, room temperature ionic liquid.

## I. INTRODUCTION

EXPOSURE to air toxins and harmful gases is an ever present concern for human health in modern society. Airborne pollutants cause discomfort, illness, and even death [1]. As these dangers to human health and safety increase, there is a growing need for miniaturized, flexible, low power, multi-gas sensor systems suitable for individuals to wear and capable of constantly examining the surrounding environment. To realize such a reliable multi-gas monitor in a wearable microsystem platform, a gas sensor array with flexibility, low cost, low power consumption, and small footprint is needed. Among the common commercial gas sensor technologies (e.g., metal oxide semiconductive [2], piezoelectric [3], surface acoustic wave [4], electrochemical [5], [6], etc), electrochemical gas sensing is the most promising choice due to its low cost, low power implementation, and outstanding performance in sensitivity and selectivity. Furthermore, the instrumentation needed for such sensors can readily be implemented as a single microelectronics chip suitable for wearable devices [7]–[9].

Recently, the use of room temperature ionic liquids (RTILs) as a sensing media [10] has drawn much attention in electrochemical gas sensing field. RTILs are nonvolatile and

conductive compounds consisting entirely of ions. With properties such as negligible vapor pressure, wide potential windows, and high thermal stability, RTILs offer a promising electrolyte for robust electrochemical gas sensors that can operate in extreme conditions. In addition, unlike conventional tin-oxide gas sensors that operate at over 200 °C [11], RTILs function at room temperature and thus greatly reduce power demands by eliminating the need to heat the sensor. Utilizing electrochemical measurement techniques, RTILs are capable of sensing a variety of environmental gases, including oxygen [12]–[17], ambient toxic gases (e.g. NO<sub>2</sub> [18], NO [19], NH<sub>3</sub> [20], H<sub>2</sub>S [21]), and volatile organic compounds (VOCs) [22], [23].

However, existing RTIL-based electrochemical gas sensors have not addressed wearable/flexible requirements. Most RTIL-based electrochemical gas sensors have adapted traditional structures such as probes [12], [13], [24], [25], Clark cells [14], and silicon substrates [16], [17], [22]. Paper-based planar sensor has been reported recently [15], [23] to provide flexibility and low cost. However, paper-based substrates are not durable and are not resistant to acidic gases. To date, no robust flexible RTIL-based gas sensors are known to have been reported.

This paper introduces a planar-electrodes-on-permeable-membrane (PEoPM) structure that enables realization of a robust flexible RTIL-based electrochemical gas sensor. Section II introduces the gas sensor structural design and material choices. Section III presents the microfabrication process for a PEoPM RTIL gas sensor. In Section IV, functionality and performance measurements of the PEoPM RTIL gas sensor are presented using oxygen as an example analyte, demonstrating high sensitivity, good linearity and repeatability.

## II. SENSOR STRUCTURE DESIGN

The first step in the design of a robust flexible RTIL sensor structure is the selection of a substrate material that meets all of these criteria: flexible, robust, inexpensive, highly sensitive, and rapid response. Porous polytetrafluoroethylene (PTFE) was chosen for the sensor structure for several reasons. First, porous PTFE is physically flexible and can be easily conformed to many surface shapes. Second, PTFE is inert to most chemicals and thus is ideal for fabricating robust gas sensors. Third, porous PTFE membrane has been widely used as a gas permeable membrane for electrochemical cells in gas sensor applications because of its relatively low cost and availability in the commercial market. Fourth, because

Manuscript received December 14, 2012; revised April 4, 2013; accepted May 3, 2013. Date of publication May 15, 2013; date of current version August 30, 2013. This work was supported in part by the Center for Disease Control, National Institute for Occupational Safety and Health under Grant R01OH009644. The associate editor coordinating the review of this paper and approving it for publication was Dr. Ravinder S. Dahiya.

X. Mu and A. J. Mason are with the Department of Electrical and Computer Engineering, Michigan State University, East Lansing, MI 48824 USA (e-mail: muxiaoyi@msu.edu; mason@msu.edu).

Z. Wang and X. Zeng are with Chemistry Department, Oakland University, Rochester, MI 48309 USA (e-mail: zhewang188@gmail.com; zeng@oakland.edu).

Color versions of one or more of the figures in this paper are available online at <http://ieeexplore.ieee.org>.

Digital Object Identifier 10.1109/JSEN.2013.2262932

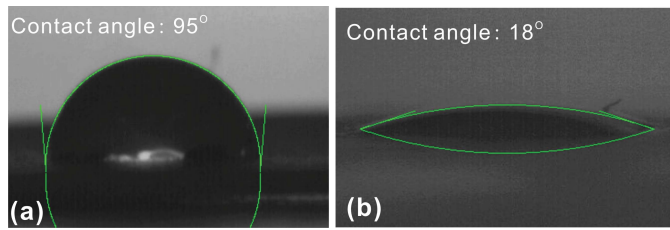


Fig. 1. (a) Contact angle of RTIL on porous PTFE. The contact angle is  $95^\circ$ , implying porous PTFE's hydrophobic response to RTIL. (b) Contact angle of RTIL on  $0.3 \mu\text{m}$ -thick gold layer coated on porous PTFE. The contact angle is  $18^\circ$ , implying gold's hydrophilic response to RTIL.

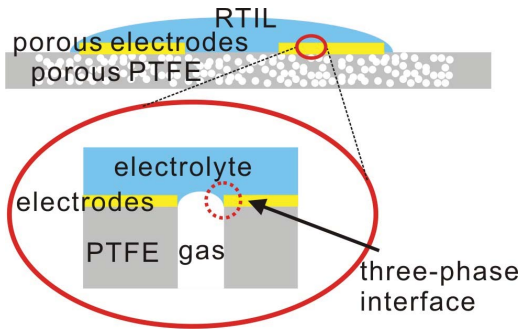


Fig. 2. PEoPM RTIL sensor structure with three-phase interface illustration.

sensor's reaction current is proportional to the electrode area and porous substrate has a high surface area, electrodes formed directly on porous substrates enable high sensitivity [26]. Fifth, because the response time of electrochemical gas sensors is directly related to the three-phase (electrolyte/electrode/gas) interface area [27], a porous and uncovered working electrode (WE) physically integrated with a porous substrate provides an ideal gas sensor design. Based on these conditions, POREX<sup>®</sup> porous PTFE with 35% porosity and  $4 \mu\text{m}$  pore size (Zitex TM, Chemplast, Incorporated, Wayne, New Jersey) was chosen for the PEoPM design in this research.

The second design step is to choose the electrode and RTIL materials. Gold was chosen as the electrode because it is highly inert and can be readily deposited in thin films. High-purity 1-butyl-1-methylpyrrolidinium bis(trifluoromethylsulfonyl)imide ( $[\text{C}_4\text{mpy}][\text{NTf}_2]$ ) RTIL was chosen as the electrolyte due to its low viscosity, high chemical stability, and its success in sensing oxygen [14].

With the materials chosen, an important property was revealed: as shown in Fig. 1, porous PTFE is hydrophobic to RTIL  $[\text{C}_4\text{mpy}][\text{NTf}_2]$  while gold on porous PTFE is hydrophilic to RTIL  $[\text{C}_4\text{mpy}][\text{NTf}_2]$ . Thus, due to surface energy difference between different materials, the designed RTIL-based sensor structure allows formation of a large three-phase interface, as illustrated in Fig. 2. To simplify the fabrication process, enable flexibility and lower cost, a planar microfabrication scheme was developed to implement this sensor structure. This results in the planar-electrodes-on-permeable-membrane (PEoPM) structure introduced by this paper.

### III. FABRICATION OF A PEOPM RTIL SENSOR

Fabrication of a PEoPM RTIL sensor follows two steps: planar electrode patterning on porous PTFE, and RTIL layer

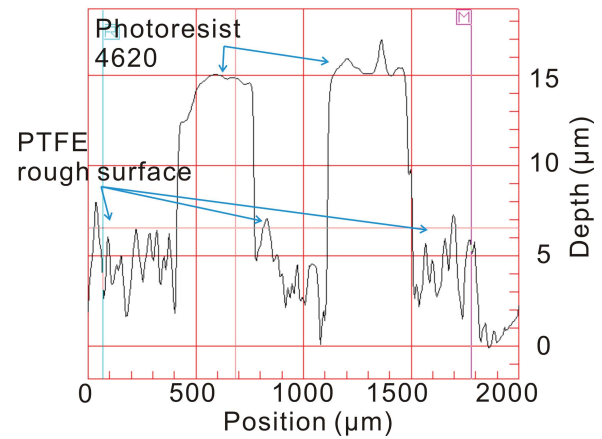


Fig. 3. Profile scan by Dektak3 Surface Profiler. The photoresist AZ4620 covered the rough surface of porous PTFE and a good step was formed.

coating on PEoPM surface. The former step can be implemented by a microfabrication process. The latter step can be implemented by a RTIL droplet process.

Microfabrication processes have been well developed and widely used in the semiconductor industry. Using photolithography followed by thermal metal deposition and the liftoff process, electrode patterns on smooth substrates can easily be formed. However, directly applying traditional photolithography on porous PTFE substrates, as desired here, introduces several problems that require development of a new photolithography process for porous substrates.

First, note that photoresist is generally spin-coated onto a substrate that is vacuum-attached to a spinner. However, porous PTFE is soft and cannot be reliably held by vacuum because it is porous. A preliminary experiment demonstrated that, when a PTFE sheet was put directly on the spinner, significant photoresist would be pulled into the PTFE and could not be removed during liftoff. To resolve this problem, the porous PTFE was clamped to a glass substrate, and the glass was placed on the spinner and held by vacuum. Second, because porous PTFE has a rough surface, standard photoresist coatings of PTFE are not reliably smooth enough for patterning. For example, with porous PTFE having a  $4 \mu\text{m}$  pore size, around  $4 \mu\text{m}$  of surface roughness can be expected. To resolve this problem, a thick film photoresist was selected. Hoechst AZ4620 was spin-coated at 2100 rpm to create  $10 \mu\text{m}$  thick layer. Lithography by 60 s UV exposure and 300 s developing in AZ300 MIF developer was found to reliably remove the thick resist. The profile scan by a Dektak3 Surface Profiler in Fig. 3 demonstrates that the photoresist AZ4620 covered the rough surfaces of porous PTFE and that a good edge step, suitable for liftoff, was formed. Finally, preliminary experiments found metal liftoff to be difficult, even after a gold-deposited sample was soaked in acetone for several days. One possible reason is that the photoresist became polymerized during the half hour physical vapor deposition, where the temperature on the sample is over  $100^\circ\text{C}$ . Because polymerized photoresist cannot easily be dissolved in acetone, this would cause the liftoff to fail. To solve this problem, exposure to UV should prevent photoresist from polymerizing.

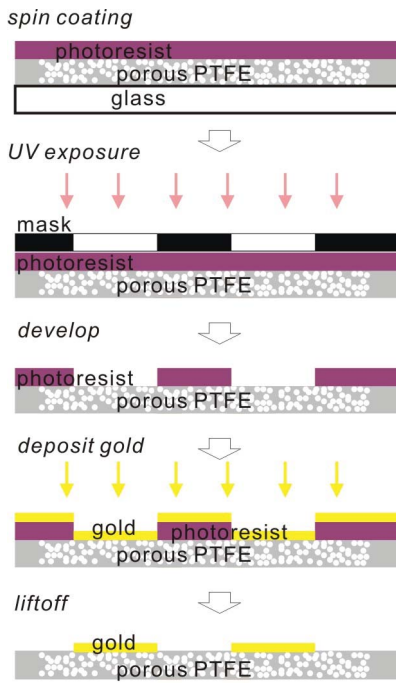


Fig. 4. PEOPM structure fabrication process.

Thus, a 60 s flood exposure was performed after developing the photoresist and before metal deposition.

By addressing each of the challenges described above, the electrode fabrication process was optimized to achieve the PEOPM structure. The fabrication process is illustrated in Fig. 4. The porous PTFE sheet was clamped on glass wafer and spin-coated by AZ4620 photoresist. 5 min soft bake at 95 °C was performed, followed by a 60 s UV exposure through the electrode pattern mask. After 300 s developing in AZ300 MIF developer, the sample was flood exposed for 60 s. Then a 300 nm-thick gold film was deposited on the porous PTFE sheet using physical vapor deposition (PVD, Edward 360 thermal evaporator). After deposition, the sample was soaked in acetone overnight and the gold electrodes pattern was formed by lift-off.

Following electrode formation, a thin gel-like RTIL layer was applied to the PEOPM sheet by a droplet process. Because RTIL has high viscosity, it would typically stick to the porous surface regardless mechanical disturbance. However, a thin layer cannot be formed by directly dropping pure RTIL on the PEOPM sheet. That's because porous PTFE is hydrophobic to RTIL (Fig. 1a), while gold on porous PTFE is hydrophilic to RTIL (Fig. 1b). The surface energy difference for different substrates results in RTIL holding on individual electrodes as "islands" when applying a small volume ( $0.2 \mu\text{L}$  in the experiment) of pure RTIL on a PEOPM sheet, as shown in Fig. 5 Case 1. If the RTIL islands become disconnected, the electrolyte fails to form an electrochemical cell over the electrodes. Although islands could merge into a bulky droplet when applying a large volume ( $1 \mu\text{L}$  in the experiment) of pure RTIL, as shown in Fig. 5 Case 2, this large droplet would easily flow away with small mechanical disturbances, ruining the sensor.

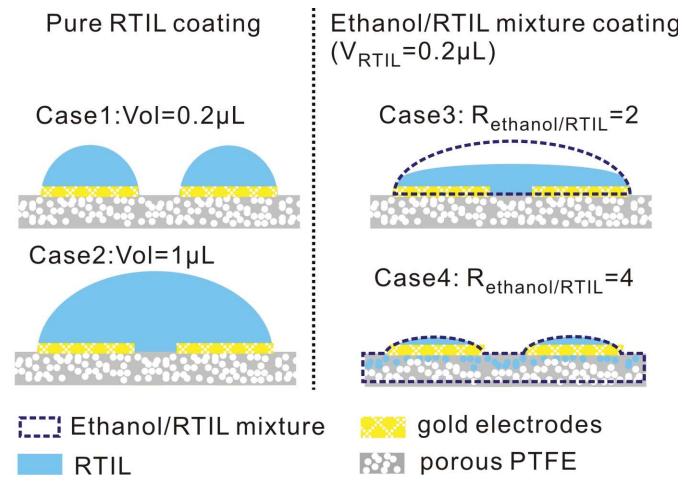


Fig. 5. Coating experiments illustration. Case1 illustrates small volume pure RTIL coating ( $\text{Vol.} = 0.2 \mu\text{L}$ ) result. RTIL droplets were coated only electrodes surface. Case2 illustrates large volume pure RTIL coating ( $\text{Vol.} = 1 \mu\text{L}$ ) result. RTIL droplets were coat electrodes surface as well as the gap between electrodes. Case3 illustrates ethanol/RTIL mixture coating ( $R_{\text{ethanol}/\text{RTIL}} = 2$ , RTIL's vol. =  $0.2 \mu\text{L}$ ) result. The initial mixture droplet was coated the electrodes area as well as the gap between electrodes. After ethanol removal, RTIL still occupied the initial droplet region. Case4 illustrates ethanol/RTIL mixture coating ( $R_{\text{ethanol}/\text{RTIL}} = 4$ , RTIL's vol. =  $0.2 \mu\text{L}$ ) result. The initial mixture droplet filled the pores inside the porous PTFE as well as covered electrodes surface. After ethanol removal, RTIL still stayed in the porous PTFE.

The problem described above results from RTIL's high surface tension on porous PTFE. Therefore, a solution is to lower the droplet's surface tension. One approach is to mix RTIL with solvents that have low surface tension on porous PTFE. Ethanol was chosen for low surface tension on porous PTFE. It can be mixed with RTIL in any ratio. In addition, ethanol can easily be removed through evaporation. By fixing the RTIL volume to  $0.2 \mu\text{L}$ , droplets with different ratios of ethanol to RTIL (denoted by  $R_{\text{ethanol}/\text{RTIL}}$ ) were dropped on the PEOPM surface, and the PEOPM sheet was then vacuumed for two hours to remove ethanol. These experiments are illustrated in Fig. 5 Case 3 and Case 4. In Case 3, the initial mixture droplet coated not only the electrode area but also the gap between electrodes in the same electrochemical cell. After ethanol removal, RTIL still occupied the initial droplet region, and a conformal thin layer of RTIL was formed on both PTFE and electrodes surface. AC impedance measurement between electrodes shows a resistance on the order of  $10^2 \Omega$ , implying good conductivity of electrolyte within the electrochemical cell. In Case 4 with higher ethanol concentration, the mixture's surface tension was too small and the droplet filled the pores inside the porous PTFE as well as covering electrode surface. After ethanol removal, RTIL still remained within the porous PTFE. AC impedance measurement between electrodes shows an open circuit. Even if the volume of the droplet was increased, a large resistance (on the order of  $10^6 \Omega$ ) was measured for this ethanol/RTIL ratio due to uneven pore distribution and limited pore connection inside the porous PTFE. Following this procedure, optimized mixing ratio ( $R_{\text{ethanol}/\text{RTIL}} = 2$ ) and droplet volume ( $V_{\text{RTIL}} = 0.2 \mu\text{L}$ ) were experimental obtained

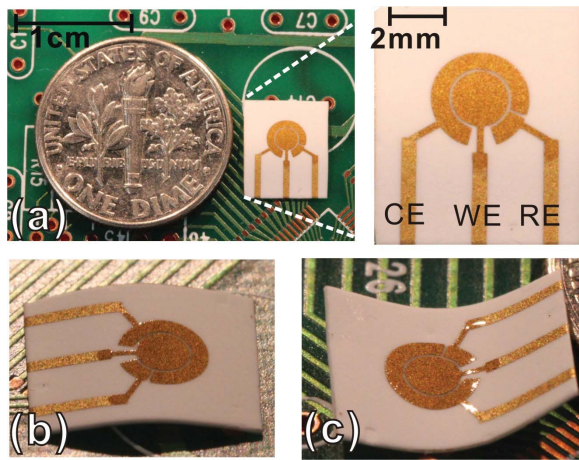


Fig. 6. (a) Photograph of microfabricated flexible PEOPM RTIL sensor. (b) Photograph of convex bend of the PEOPM RTIL sensor. (c) Photograph of concave bend of the PEOPM RTIL sensor.

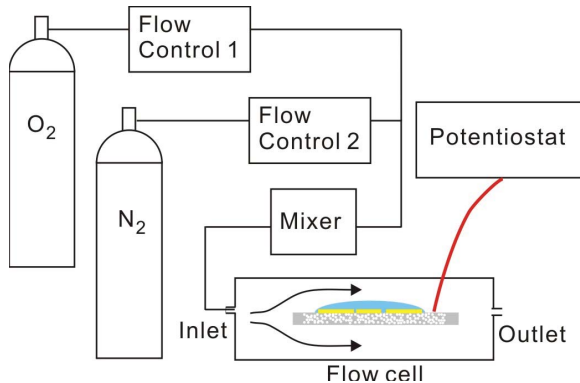


Fig. 7. Gas test setup and position of the sensor within the flow cell.

to form a thin and conformal layer on the PEOPM surface that achieved a good, conductive electrochemical cell.

After the microfabrication and droplet processes above, the PEOPM RTIL sensor shown in Fig. 6(a) was produced. A disk-shaped WE with radius of 1 mm was patterned in the center of porous PTFE sheet. An annular counter electrode (CE) with inner radius of 1.125 mm and outer radius of 1.75 mm and a reference electrode (RE) were patterned around the WE. The gap between WE and CE is 125  $\mu\text{m}$ . The total sensing region occupies 9.6  $\text{mm}^2$ . A 21  $\mu\text{m}$ -thick  $[\text{C}_4\text{mpy}][\text{NTf}_2]$  layer was coated on the sensing region, covering all electrodes and the gaps between them. The resulting sensor structure can be bent either convex or concave as shown in Fig. 6, demonstrating its physical flexibility.

## IV. RESULTS

### A. Test Setup

Chemical experiments were carried out using the test setup as shown in Fig. 7. Oxygen was selected as an example analyte. Oxygen and nitrogen (as background gas) concentrations were controlled using digital mass-flow controllers (MKS Instruments, Inc.) to vary oxygen concentration from 0% to 21%. The total flow rate was fixed to 100 standard cubic centimeters per minute (scm) to circumvent the influence of differential gas flow rate. The PEOPM RTIL sensor was placed

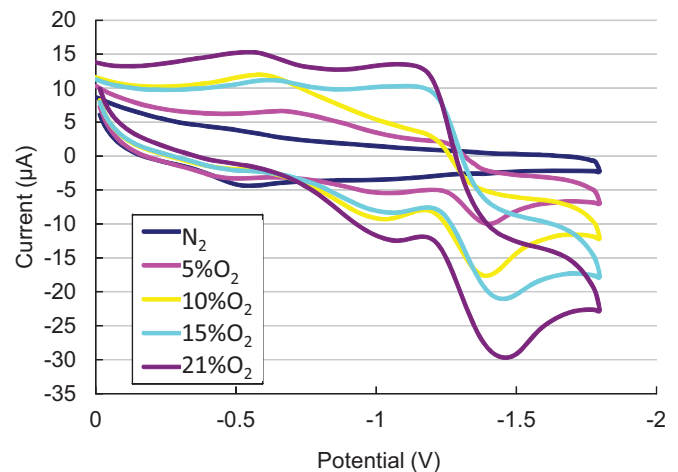


Fig. 8. Cyclic voltammograms (scan rate = 500 mV/s) for the reduction of oxygen at WE. Oxygen concentration varies from 0%–21%. Oxygen reduction current peak was observed at  $-1.4$  V vs Au. The relationship between peak current and oxygen concentration from 0% to 21% is linear.

in a flow cell within a desiccant gas chamber parallel to the gas flow as shown in Fig. 7. The gas flows across both side of the sensor and reaches the electrodes both by permeating through porous PTFE and by dissolving into RTIL. However, based on previously reported experiments [28], the response time is determined by the faster path permeating through the porous PTFE. Through wires that were attached to the sensor pads with conductive epoxy, the sensor was connected to a VersaStatMC potentiostat (Princeton Applied Research, Oak ridge, TN, U.S.A) for electrochemical test.

### B. Experimental Results

To verify the functionality of the PEOPM RTIL sensor, cyclic voltammetry (CV) was performed between  $-1.8$  V and 0 V with 500 mV/s scan rate for the reduction of oxygen at the WE, as shown in Fig. 8 where the oxygen concentration ranges from 0% to 21%. A broad current peak was observed at about  $-1.4$  V vs Au, which is in agreement with the CVs obtained for oxygen reduction in RTIL reported in [14]. The relationship between peak current  $I_p$  ( $\mu\text{A}$ ) and oxygen concentration  $C_{\text{O}_2}$  (%) was found to fit the following linear calibration condition

$$I_p = -1.25 C_{\text{O}_2} - 3.35 (R^2 = 0.989). \quad (1)$$

This relationship demonstrates the functionality and linearity of the PEOPM RTIL sensor.

For real-time monitoring, the constant-potential amperometry method is usually used due to its simple hardware implementation. To characterize the performance of the PEOPM RTIL sensor using constant-potential amperometry, the sensor was biased at the oxygen reduction potential of  $-1.4$  V and the current was measured. The sensor's sensitivity, linearity, repeatability and limit of detection (LOD) were characterized as follows.

The sensor's response linearity was characterized by a step change of oxygen concentration from 0% to 21% and then back to 0%. The response current vs. time curve shown in Fig. 9 was recorded. The stable values at each step were

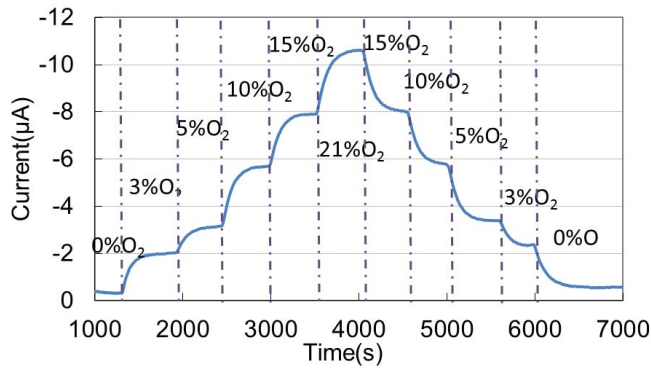


Fig. 9. Current versus time curve at various oxygen concentrations when the potential is held at  $-1.4$  V vs Au. Nitrogen is the background gas. Oxygen concentration steps up from 0% to 21% and steps down from 21% to 0%.

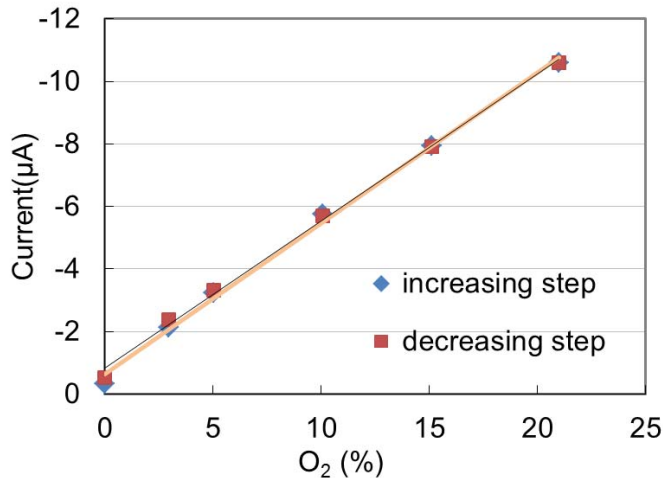


Fig. 10. Oxygen calibration curve for RTIL sensor using data extracted from Fig. 9.

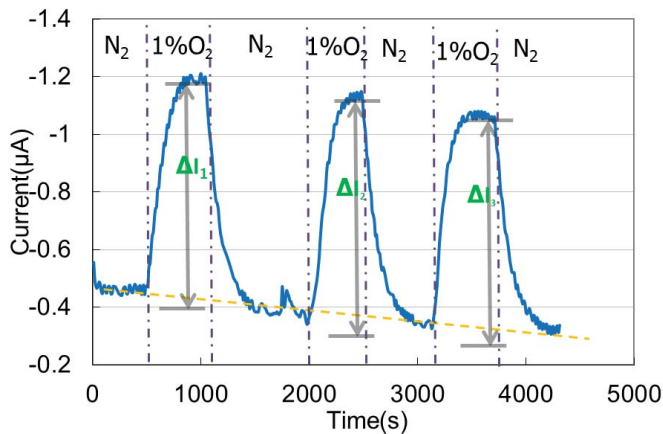


Fig. 11. Constant-potential current response measured over three cycles of alternate exposure to 1% oxygen and pure nitrogen flow at an applied potential of  $-1.4$  V.

collected to form the oxygen calibration curve shown in Fig. 10. The relationship between amperometric current  $I_a$  ( $\mu\text{A}$ ) and oxygen concentration  $C_{O_2}$  (%) can be expressed by

$$I_a = -0.48 C_{O_2} - 0.64 (R^2 = 0.997). \quad (2)$$

The sensitivity of the amperometric response was measured as  $0.48 \mu\text{A}/\%$ . The  $R^2$  value of 0.997 implies a good linearity of the sensor response to oxygen.

Repeatability test was performed by alternately purging 1% oxygen and pure nitrogen. The resulting amperometric current is shown in Fig. 11. Although the sensor shows a slight drift due to decay of the double layer capacitor charging current, by subtracting the baseline value the response current  $\Delta I$  shows a good repeatability with an average value of  $0.73 \mu\text{A}$  and a standard deviation of only  $1.5 \text{ nA}$ . The corresponding LOD for oxygen, defined as three times of the baseline noise or  $0.038 \mu\text{A}$ , was found to be  $0.08 \text{ vol } \%$ .

## V. CONCLUSION

This paper introduced the realization of a robust flexible RTIL electrochemical gas sensor featuring a planar-electrode-on-permeable-membrane structure that provides flexibility, high sensitivity and fast response. Using oxygen as an example analyte, the sensor's functionality and performance was demonstrated. Using oxygen as an example analyte, the sensor achieves a sensitivity of  $0.48 \mu\text{A}/\%O_2$ , a linearity of 0.997  $R^2$  value in range of 0%–21%  $O_2$ , and LOD of 0.08%. By modifying applied electrochemical potential and RTIL material, sensing of other gases can be readily achieved. The reported microfabrication process enables future realization of miniaturized sensor arrays for wearable multi-gas monitoring microsystems.

## REFERENCES

- [1] R. D. Brook, "Cardiovascular effects of air pollution," *Clinical Sci.*, vol. 115, no. 6, pp. 175–187, Sep. 2008.
- [2] C. O. Park and S. A. Akbar, "Ceramics for chemical sensing," *J. Mater. Sci.*, vol. 38, no. 23, pp. 4611–4637, 2003.
- [3] L. Yu, D. Garcia, R. Ren, and X. Zeng, "Ionic liquid high temperature gas sensors," *Chem. Commun.*, vol. 17, pp. 2277–2279, Jan. 2005.
- [4] C.-S. Chiu and S. Gwo, "Quantitative surface acoustic wave detection based on colloidal gold nanoparticles and their bioconjugates," *Anal. Chem.*, vol. 80, no. 9, pp. 3318–3326, May 2008.
- [5] J. R. Stetter, G. Korotcenkov, X. Zeng, Y. Tang, and Y. Liu, "Electrochemical gas sensors: Fundamentals, fabrication, and parameters," in *Chemical Sensors Comprehensive Sensor Technologies*, vol. 5, G. Korotcenkov, Ed. New York, NY, USA: Momentum Press, 2011, pp. 1–89.
- [6] J. R. Stetter and J. Li, "Amperometric gas sensors—A review," *Chem. Rev.*, vol. 108, no. 2, pp. 352–366, Jan. 2008.
- [7] A. Manickam, A. Chevalier, M. McDermott, A. D. Ellington, and A. Hassibi, "A CMOS electrochemical impedance spectroscopy (EIS) biosensor array," *IEEE Trans. Biomed. Circuits Syst.*, vol. 4, no. 6, pp. 379–390, Nov. 2010.
- [8] P. M. Levine, G. Ping, R. Levicky, and K. L. Shepard, "Active CMOS sensor array for electrochemical biomolecular detection," *IEEE J. Solid-State Circuits*, vol. 43, no. 8, pp. 1859–1871, Aug. 2008.
- [9] Y. Chao, S. R. Jadhav, R. M. Worden, and A. J. Mason, "Compact low-power impedance-to-digital converter for sensor array microsystems," *IEEE J. Solid-State Circuits*, vol. 44, no. 10, pp. 2844–2855, Oct. 2009.
- [10] E. I. Rogers, A. M. O'Mahony, L. Aldous, and R. G. Compton, "Amperometric gas detection using room temperature ionic liquid solvents," *ECS Trans.*, vol. 33, pp. 473–502, Jan. 2010.
- [11] J. Watson, K. Ihokura, and G. S. V. Coles, "The tin dioxide gas sensor," *Meas. Sci. Technol.*, vol. 4, no. 7, pp. 710–711, 1993.
- [12] R. Toniolo, N. Dossi, A. Pizzariello, A. P. Doherty, S. Susmel, and G. Bontempelli, "An oxygen amperometric gas sensor based on its electrocatalytic reduction in room temperature ionic liquids," *J. Electroanal. Chem.*, vol. 670, no. 1, pp. 23–29, Apr. 2012.

- [13] R. Wang, T. Okajima, F. Kitamura, and T. Ohsaka, "A novel amperometric O<sub>2</sub> gas sensor based on supported room-temperature ionic liquid porous polyethylene membrane-coated electrodes," *Electroanalysis*, vol. 16, nos. 1–2, pp. 66–72, Jan. 2004.
- [14] Z. Wang, P. Lin, G. A. Baker, J. Stetter, and X. Zeng, "Ionic liquids as electrolytes for the development of a robust amperometric oxygen sensor," *Anal. Chem.*, vol. 83, no. 18, pp. 7066–7073, Aug. 2011.
- [15] C. Hu, X. Bai, Y. Wang, W. Jin, X. Zhang, and S. Hu, "Inkjet printing of nanoporous gold electrode arrays on cellulose membranes for high-sensitive paper-like electrochemical oxygen sensors using ionic liquid electrolytes," *Anal. Chem.*, vol. 84, no. 18, pp. 3745–3750, Mar. 2012.
- [16] X.-J. Huang, L. Aldous, A. M. O'Mahony, F. J. Del Campo, and R. G. Compton, "Toward membrane-free amperometric gas sensors: A microelectrode array approach," *Anal. Chem.*, vol. 82, no. 12, pp. 5238–5245, May 2010.
- [17] S.-Q. Xiong, Y. Wei, Z. Guo, X. Chen, J. Wang, J.-H. Liu, and X. J. Huang, "Toward membrane-free amperometric gas sensors: An ionic liquid–nanoparticle composite approach," *J. Phys. Chem. C*, vol. 115, no. 35, pp. 17471–17478, Aug. 2011.
- [18] M. Nádherná, F. Opekar, and J. Reiter, "Ionic liquid–polymer electrolyte for amperometric solid-state no<sub>2</sub> sensor," *Electrochim. Acta*, vol. 56, pp. 5650–5655, Apr. 2011.
- [19] S. R. Ng, C. X. Guo, and C. M. Li, "Highly sensitive nitric oxide sensing using three-dimensional graphene/ionic liquid nanocomposite," *Electroanalysis*, vol. 23, no. 2, pp. 442–448, 2011.
- [20] X. Ji, C. E. Banks, D. S. Silvester, L. Aldous, C. Hardacre, and R. G. Compton, "Electrochemical ammonia gas sensing in nonaqueous systems: A comparison of propylene carbonate with room temperature ionic liquids," *Electroanalysis*, vol. 19, no. 21, pp. 2194–2201, 2007.
- [21] A. M. O'Mahony, D. S. Silvester, L. Aldous, C. Hardacre, and R. G. Compton, "The electrochemical reduction of hydrogen sulfide on platinum in several room temperature ionic liquids," *J. Phys. Chem. C*, vol. 112, no. 20, pp. 7725–7730, 2008.
- [22] M. A. G. Zevenbergen, D. Wouters, V.-A. T. Dam, S. H. Brongersma, and M. Crego-Calama, "Electrochemical sensing of ethylene employing a thin ionic-liquid layer," *Anal. Chem.*, vol. 83, no. 16, pp. 6300–6307, 2011.
- [23] N. Dossi, R. Toniolo, A. Pizzariello, E. Carrilho, E. Piccin, S. Battiston, and G. Bontempelli, "An electrochemical gas sensor based on paper supported room temperature ionic liquids," *Lab Chip*, vol. 12, no. 1, pp. 153–158, 2012.
- [24] R. Toniolo, N. Dossi, A. Pizzariello, A. P. Doherty, and G. Bontempelli, "A membrane free amperometric gas sensor based on room temperature ionic liquids for the selective monitoring of NO<sub>x</sub>," *Electroanalysis*, vol. 24, no. 4, pp. 865–871, 2012.
- [25] R. Toniolo, A. Pizzariello, S. Susmel, N. Dossi, A. P. Doherty, and G. Bontempelli, "An ionic-liquid based probe for the sequential preconcentration from headspace and direct voltammetric detection of phenols in wastewaters," *Electroanalysis*, vol. 19, nos. 19–20, pp. 2141–2148, 2007.
- [26] M. Wienecke, M.-C. Bunescu, M. Pietrzak, K. Deistung, and P. Fedtke, "PTFE membrane electrodes with increased sensitivity for gas sensor applications," *Synth. Met.*, vol. 138, no. 1, pp. 165–171, 2003.
- [27] M. C. Simmonds, M. L. Hitchman, H. Kheyrandish, J. S. Colligon, N. J. Cade, and P. J. Iredale, "Thin Sputtered Platinum Films on Porous Membranes as Working Electrodes in Gas Sensors," *Electrochim. Acta*, vol. 43, nos. 21–22, pp. 3285–3291, 1998.
- [28] X. Mu, Z. Wang, M. Guo, X. Zeng, and A. J. Mason, "Fabrication of a miniaturized room temperature ionic liquid gas sensor for human health and safety monitoring," in *Proc. IEEE Biomed. Circuits Syst. Conf.*, Nov. 2012, pp. 140–143.



**Xiaoyi Mu** (S'11) received the B.S. and M.S. degree in materials science from Fudan University, Shanghai, China, in 2004 and 2007, respectively, and the M.S. degree in electrical engineering from Michigan State University, East Lansing, MI, USA, in 2010. Currently, he is pursuing the Ph.D. degree in electrical engineering at Michigan State University. From 2007 to 2008, he was a Circuit Design Engineer with Integrated Device Technology Inc., Shanghai Design Center, Shanghai. His current research interests include the analog and mixed-signal IC design

for sensor interface, electrochemical sensor development, and electrochemical microsystem integration.



**Zhe Wang** received the B.S. and Ph.D. degrees in analytical chemistry from Lanzhou University, Lanzhou, China, in 2001 and 2007, respectively. He was a Post-Doctoral Researcher with the University of California at Los Angeles, Los Angeles, CA, USA, from 2007 to 2009. Currently, he is with the Chemistry Department, Oakland University, Rochester, MI, USA, as a Post-Doctoral Researcher. His current research interests include electrochemistry and material science, the study of gas electrochemical properties for chemical and biosensors based on ionic liquids and nanomaterials, and the development of multifunctional nanomaterials. He has published over 30 peer reviewed publications. He is the member of AICHE, ECS, MRS, ACS, ASC, ANS, and SAMPE. He was a Chair of Functional Nanoparticles and Nanocoatings on Particles I and II Session in AICHE Annual Meeting 2011. He received the Outstanding Researcher Award of Oakland University in 2010 and 2011 and the Excellent Graduated Student Award, Lanzhou University.



**Xiangqun Zeng** received the B.S. degree from the Chengdu University of Science and Technology (now Si Chuan University), Chengdu, China, in 1989, the M.S. degree from Beijing Normal University, Beijing, China, in 1992, and the Ph.D. degree in electrochemistry and surface chemistry from the State University of New York at Buffalo, Buffalo, NY, USA, in 1997. She is currently a Professor with the Chemistry Department, Oakland University, Rochester, MI, USA. Her current research interests include electrochemistry and interface chemistry at

solid electrodes, the development of new analytical techniques, chemical and biosensors, ionic liquids, and conductive polymers. She has published over 50 peer reviewed publications and she is currently holds five patents. She is the Chair of chemistry's graduate studies committee as well as a Program Director for the Ph.D. and M.S. programs with the Chemistry Department, Oakland University. She received the Oakland University Young Investigator Research Excellence Award in 2005 and the Academic Excellence Recognition Award in 2011 and 2012.



**Andrew J. Mason** (S'90–M'99–SM'06) received the B.S. degree (Hons.) in physics from Western Kentucky University, Bowling Green, KY, USA, in 1991, the B.S.E.E. degree (Hons.) from the Georgia Institute of Technology, Atlanta, GA, USA, in 1992, and the M.S. and Ph.D. degrees in electrical engineering from the University of Michigan, Ann Arbor, MI, USA, in 1994 and 2000, respectively. He is currently an Associate Professor with the Department of Electrical and Computer Engineering, Michigan State University, East Lansing, MI, USA. His current

research interests include mixed-signal circuits and microfabricated structures for integrated microsystems in biomedical and environmental monitoring applications. His current projects include wearable/implantable electrochemical and bioelectronic sensors systems, microfabricated electrochemical sensor arrays, array signal processing algorithms and hardware, and post-CMOS integration of sensing, instrumentation, and microfluidics. He is an Associate Editor for two professional journals, and he was Co-General Chair of the 2011 IEEE Biomedical Circuits and Systems Conference. He is a recipient of the 2006 Michigan State University Teacher-Scholar Award and the 2010 Withrow Award for Teaching Excellence.